Integration and Modularity of Quantitative Trait Locus Effects on Geometric Shape in the Mouse Mandible

Christian Peter Klingenberg,*,[1] Larry J. Leamy[†] and James M. Cheverud[‡]

School of Biological Sciences, University of Manchester, Manchester M13 9PT, United Kingdom, [†]Department of Biology, University of North Carolina, Charlotte, North Carolina 28223 and [‡]Department of Anatomy and Neurobiology, Washington University School of Medicine, Saint Louis, Missouri 63110

Manuscript received September 9, 2003
Accepted for publication December 23, 2003

ABSTRACT

The mouse mandible has long served as a model system for complex morphological structures. Here we use new methodology based on geometric morphometrics to test the hypothesis that the mandible consists of two main modules, the alveolar region and the ascending ramus, and that this modularity is reflected in the effects of quantitative trait loci (QTL). The shape of each mandible was analyzed by the positions of 16 morphological landmarks and these data were analyzed using Procrustes analysis. Interval mapping in the F_2 generation from intercrosses of the LG/J and SM/J strains revealed 33 QTL affecting mandible shape. The QTL effects corresponded to a variety of shape changes, but ordination or a parametric bootstrap test of clustering did not reveal any distinct groups of QTL that would affect primarily one module or the other. The correlations of landmark positions between the two modules tended to be lower than the correlations between arbitrary subsets of landmarks, indicating that the modules were relatively independent of each other and confirming the hypothesized location of the boundary between them. While these results are in agreement with the hypothesis of modularity, they also underscore that modularity is a question of the relative degrees to which QTL contribute to different traits, rather than a question of discrete sets of QTL contributing to discrete sets of traits.

ORGANISMAL form is a composite of many constituent parts, and even single morphological structures may be assembled from multiple parts that have different embryonic origins or fulfill different functions. To understand such complex morphological structures, it is important to know to which degree they are integrated as a whole or subdivided into partially autonomous modules that may correspond to functional or developmental subunits (Cheverud 1996; Wagner 1996). Modules are units that are internally coherent due to strong interconnection among their parts and relatively independent of other such units within a larger system. For the genetic architecture of a modular structure, this implies that pleiotropic effects should be concentrated within modules but relatively weak among modules (Cheverud 1996; Wagner 1996; Wagner and Altenberg 1996; von Dassow and Munro 1999). The developmental processes that produce the structure are prime factors mediating modularity and its effects on genetic architecture (Riska 1986; Cheverud 1996; Hall 1999; Davidson 2001; Klingenberg 2004).

The mouse mandible has long served as a model system for complex structures and has contributed significantly to an improved understanding of the genetic and developmental determinants of morphological variation in general (Atchley and Hall 1991; Cheverud *et al.* 1991; Hall 1999, Chap. 20). The mandible originates from neural crest cells in a sequence of interactive processes that produce its elaborate spatial pattern (Trainor and Tam 1995; Miyake *et al.* 1997; Tomo *et al.* 1997; Chai *et al.* 2000; Ferguson *et al.* 2000; Depew *et al.* 2002a,b; Cobourne and Sharpe 2003; Ramaesh and Bard 2003). Various signaling mechanisms take part in this process and may contribute to the overall integration of the final structure (Francis-West *et al.* 1998; Depew *et al.* 2002b; Cobourne and Sharpe 2003). While the genes known to be involved in these signaling cascades are possible candidates for loci that affect morphological integration, a host of other mechanisms may also contribute to it, and any locus with pleiotropic effects on multiple parts of the mandible has the potential to affect the integration among them (Cheverud 1996; Wagner 1996; Klingenberg 2004). Therefore, it is advantageous to investigate the genetic basis of integration and modularity with an approach that uses the observed phenotypic effects as a point of departure.

A range of new possibilities for investigating the genetic basis of integration and modularity of complex morphological structures has become available through the methods for locating quantitative trait loci (QTL; *e.g.*, Lynch and Walsh 1998; Mackay 2001; Weller 2001). Several studies have examined the spatial distribution of pleiotropic effects of QTL on measurements

[1]*Corresponding author:* School of Biological Sciences, University of Manchester, 3.614 Stopford Bldg., Oxford Rd., Manchester M13 9PT, United Kingdom. E-mail: cpk@man.ac.uk

taken in different parts of the mouse mandible (Bailey 1985, 1986; Cheverud *et al.* 1997; Mezey *et al.* 2000; Ehrich *et al.* 2003). A different strategy is to examine the integration among traits by analyzing the covariation among traits, as has been done for phenotypic and genetic components of variation in populations (Cheverud 1982; Leamy and Atchley 1984; Leamy 1993; Cheverud 1995; Klingenberg and Leamy 2001; Klingenberg *et al.* 2003). This approach can also be applied to analyze the patterns of effects of individual QTL on multiple traits. Multivariate methods for estimating patterns of QTL effects have been used to analyze covariation of different sets of distance measurements (Leamy *et al.* 1999; Ehrich *et al.* 2003) and inherently multidimensional phenotypes such as geometric shape (Klingenberg *et al.* 2001; Workman *et al.* 2002).

Here we use an explicitly geometric approach to reassess the hypothesis that QTL effects on the mandible are modular, that is, that separate sets of QTL tend to affect either the alveolar region or the ascending ramus (Figure 1; Cheverud *et al.* 1997; Mezey *et al.* 2000; Ehrich *et al.* 2003). We analyze the shape changes corresponding to the QTL effects and interpret them in direct relation to the anatomy of the mandible to assess the degree to which they are localized to these two regions. We also examine how the QTL effects are distributed in the multidimensional shape space to test whether there are distinct clusters of QTL according to their effects on the different parts of the mandible. Finally, as an explicit test of the hypothesized location of the boundary between modules, we compare the covariation between the alveolar region and ascending ramus with other possible partitions of the mandible into two sets of landmarks. These analyses add to and refine the methodology introduced in previous QTL analyses of shape (Klingenberg *et al.* 2001; Workman *et al.* 2002). The results shed new light on the hypothesis of modularity of QTL effects in the mandible, which we discuss in relation to the developmental mechanisms involved and the implications for genetic variation of complex morphological structures.

MATERIALS AND METHODS

Experimental design and data acquisition: This study is based on the analysis of the F_2 generation from a cross between the Jackson Laboratory Large (LG/J) and Small (SM/J) inbred strains (Cheverud *et al.* 1996; Vaughn *et al.* 1999). The analysis combines the data from two intercross experiments that were carried out separately, each consisting of >500 F_2 individuals (for details, see Vaughn *et al.* 1999). The two intercross experiments used slightly different sets of microsatellite markers that covered all 19 autosomes. For intercross 1, there were 75 polymorphic markers in 55 intervals, whereas for intercross 2 there were 96 markers in 72 intervals (for further details and a genetic map, see Vaughn *et al.* 1999, Figure 1).

The mandibles were exposed to dermestid beetles, cleaned, and the coordinates of 16 landmark points were digitized for the right hemimandible (Figure 1). In the data set for the F_2 generation from both intercrosses combined, complete data were available for the mandibles of 954 mice.

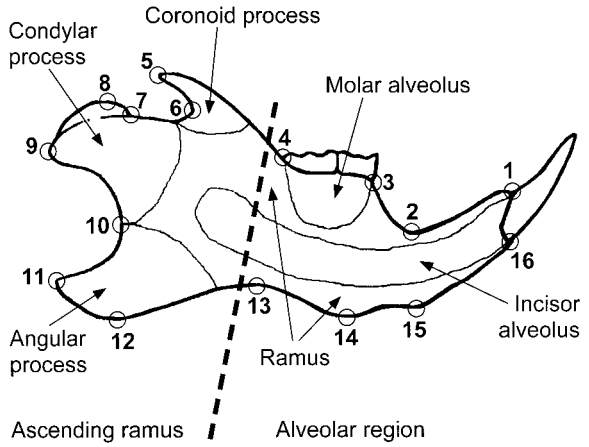

Figure 1.—Anatomical parts of the mandible and landmarks used in this study. The dashed line indicates the boundary between the alveolar region and the ascending ramus, which are hypothesized to be the primary developmental modules in the mandible (Cheverud *et al.* 1997; Mezey *et al.* 2000; Klingenberg *et al.* 2003).

Statistical analysis of shape: This study uses the methods of geometric morphometrics, which are based on an explicitly geometric definition of shape as all those features of a landmark configuration that are invariant to size, position, and orientation (Bookstein 1991; Dryden and Mardia 1998). The size measure most widely used in geometric morphometrics is centroid size, which is the square root of the sum of squared distances of the landmarks of a configuration from their center of gravity (*e.g.*, Dryden and Mardia 1998, p. 24). To extract the shape information, the landmark configurations were superimposed by generalized least-squares Procrustes superimposition and projected onto the shape tangent space at the mean shape (Dryden and Mardia 1998; Rohlf 1999). The Procrustes method scales all the landmark configurations to unit centroid size, translates them so that they have a common center of gravity, and rotates them to an optimal fit according to a least-squares criterion (*e.g.*, Klingenberg and McIntyre 1998). The variation remaining in the coordinates of superimposed landmark configurations contains the complete information about shape variation. The projection to the tangent space (*e.g.*, Rohlf 1999) is analogous to the projection of the curved surface of the earth onto a flat map, because it renders linear the constraints imposed by the Procrustes fit. Given the small amounts of shape variation in this analysis of intraspecific variation, the changes by this projection are extremely small and their effects on the results are negligible.

The coordinates resulting from the Procrustes superimposition of configurations and projection to tangent space can be analyzed with the methods of multivariate statistics. For some procedures, such as canonical correlation (see below), adjustments need to be made because the covariance matrices of the Procrustes-aligned coordinates are not of full rank. Although there are 32 coordinates for the set of 16 landmarks in 2 dimensions, the resulting shape tangent space has only 28 dimensions because 4 d.f. are lost in the Procrustes superimposition: one for size, two for position, and one for orientation (*i.e.*, 4 dimensions are redundant). A simple solution to obtain the appropriate dimensionality is to omit 4 coordinates (Bookstein 1996, p. 140; Dryden and Mardia 1998, p. 152),

which we did for the canonical correlation analysis for locating QTL (for further details, see Klingenberg *et al.* 2001; Workman *et al.* 2002). For analyses such as canonical correlation, where the effects of interest are scaled relative to within-sample variation, this method has the same effect as other methods for adjusting dimensionality, such as using generalized inverses (Dryden and Mardia 1998, p. 152). The complete set of landmark coordinates was used for estimating the QTL effects by multivariate regression and all subsequent analyses.

Before the QTL mapping, the data were corrected for the effects of sex, dam, block, and litter size (Cheverud *et al.* 1996) as well as the effect of the intercross. The data used in the subsequent analyses therefore correspond to the residuals from a linear model including all these effects.

Interval mapping and estimation of QTL effects: Interval mapping was carried out for the complete data set, combining the two intercrosses. Because each intercross used a slightly different set of microsatellite loci, genotypes at missing marker loci were inferred from flanking markers using the Mapmaker 3.0b software (Lander *et al.* 1987; Lincoln *et al.* 1992).

Because shape is an inherently multidimensional phenotype, we used a fully multivariate approach for interval mapping of QTL affecting shape. We applied the method proposed by Leamy *et al.* (1999) for interval mapping of multivariate phenotypes, which is a generalization of the univariate method of Haley and Knott (1992) and is similar to the multivariate least-squares method described by Knott and Haley (2000). At the location of the markers, additive genotypic scores were set to −1, 0, and 1 and dominance genotypic scores were set to 0, 1, and 0, respectively, for the SM/J homozygotes, heterozygotes, and LG/J homozygotes. For locations between markers, at intervals of 2 cM, these scores were computed from genotype probabilities inferred with the Mapmaker 3.0b program (Lander *et al.* 1987; Lincoln *et al.* 1992). At each location, the additive and dominance genotype scores were related to the shape variables by canonial correlation (*e.g.*, Mardia *et al.* 1979), and an approximate LOD statistic was computed (Leamy *et al.* 1999, 2000). Statistical significance of the approximate LOD scores was assessed with a permutation approach (Churchill and Doerge 1994), which was used to determine empirical significance thresholds for each chromosome separately as well as for joint genome-wide tests (for details, see Klingenberg *et al.* 2001; Workman *et al.* 2002). Confidence intervals for QTL locations were established using the one-LOD rule (Lynch and Walsh 1998).

In these analyses, the effects of QTL on other chromosomes were taken into account by conditioning on marker loci (Jansen 1993; Zeng 1994). For each chromosome for which a QTL was found, we tested for the presence of a second QTL (Leamy *et al.* 1999; Klingenberg *et al.* 2001; Workman *et al.* 2002). We tested for sex-specific QTL effects by scanning for interaction of sex with additive and dominance effects (parceling out the main effects due to genotypic values, sex, and the appropriate conditioning variables). For chromosomes with significant sex interactions, QTL were mapped in separate analyses for males and females.

For each QTL with statistically significant overall effect, the additive and dominance effects of the QTL were estimated by means of multivariate regressions of the complete set of landmark coordinates on the additive and on the dominance genotypic scores (for details, see Klingenberg *et al.* 2001; Workman *et al.* 2002). The results of these analyses are two sets of regression coefficients for each QTL, the vectors of additive effects (**a**) and dominance effects (**d**), which are the multivariate equivalents to the *a* and *d* coefficients in univariate QTL analyses (*e.g.*, Falconer and Mackay 1996). Because the entire procedure of interval mapping and estimation of QTL effects was fully multivariate, these **a** and **d** vectors can vary in both direction and magnitude, depending on the locations of genotypic means in shape space. We emphasize that this procedure does not make an *a priori* choice of shape variable before the interval mapping analyses.

In QTL analyses of shape, the **a** and **d** vectors are vectors in shape tangent space (Rohlf 1999) and therefore are amenable to the techniques for analysis and graphical presentation that are used in geometric morphometrics. The length of the vectors [*e.g.*, $||\mathbf{a}|| = (\mathbf{a}'\mathbf{a})^{0.5}$, where the prime denotes vector transposition] indicates the magnitude of the additive or dominance effect, measured in units of Procrustes chord distance (*e.g.*, Dryden and Mardia 1998). The direction of each **a** and **d** vector corresponds to the specific pattern of relative changes of landmark positions for the corresponding QTL effect. The **a** and **d** vectors were visualized by deformations of the outline of a mandible using the thin-plate spline interpolation (Bookstein 1989, 1991) and subjected to further multivariate analyses focusing on specific aspects of integration and modularity of QTL effects. We decided to include the **a** and **d** vectors of all QTL with significant overall effects in the further multivariate analyses, even if tests for individual effects were not statistically significant. The reason for this was the limited statistical power of these tests, particularly for the **d** vectors (for all but one QTL, the tests for dominance were only significant where $||\mathbf{d}|| > ||\mathbf{a}||$), but we need to point out that the multivariate analyses of the **d** vectors need to be interpreted with some caution.

Analyses of integration and modularity of QTL effects: Hypotheses about morphological integration and modularity of QTL effects concern the patterns of coordinated shifts of landmark positions for each QTL or the sets of QTL that have effects on landmarks belonging to the modules (Cheverud 1996; Wagner 1996; Wagner and Altenberg 1996; Klingenberg *et al.* 2003). These patterns can be examined by multivariate analyses of variation among the **a** and **d** vectors. We used a combination of analyses to test different aspects of the hypothesis that the alveolar region and the ascending ramus are the two primary modules of the mandible (Figure 1; *e.g.*, Cheverud *et al.* 1997; Mezey *et al.* 2000; Ehrich *et al.* 2003). Some of these analyses explored the distribution of QTL in the multidimensional space defined by the **a** or **d** vectors, whereas others focused directly on the geometry of mandible shape changes induced by the QTL. Both approaches are complementary in that they provide information on different aspects of integration and modularity of QTL effects.

Distribution of QTL effects in shape space: Cheverud *et al.* (1997; see also Ehrich *et al.* 2003) investigated how the statistically significant effects of QTL on interlandmark distances were distributed across the mandible. They found that many QTL had effects that were concentrated in either the ascending ramus or the alveolar region, but that only relatively few QTL had significant effects on both regions simultaneously. This conclusion was confirmed by a more formal statistical analysis (Mezey *et al.* 2000).

This finding that QTL tend to fall into groups according to their effects on different parts of the mandible may reflect differences in the distributions of the QTL effects in shape space. One possibility is that the **a** or **d** vectors form distinct clusters of QTL corresponding to those groups. Such clustering of QTL effects may arise as a consequence of developmental interactions of the pathways in which the respective genes take part, that is, epigenetic interactions that impart similar patterns of phenotypic effects on multiple QTL (Riska 1986; Klingenberg 2004). The alternative is that there is no clustering, but that the QTL effects are dispersed over orthogonal subspaces of shape tangent space that correspond to the modules. The two scenarios are different in their implications for the cumulative effects of QTL on the total genetic

variation, because clustered QTL effects would lead to greater stability of patterns of overall integration when allele frequencies at the QTL change (Klingenberg 2004). It is not entirely clear whether the two-module hypothesis implies two clusters, corresponding to the QTL with effects on the ascending ramus and on the alveolar region, respectively, or whether there might be an additional third cluster consisting of those QTL that have simultaneous effects on the entire mandible (Cheverud *et al.* 1997; Ehrich *et al.* 2003). Accordingly, we conducted tests for the presence of either two or three clusters among the additive and dominance effects of the QTL.

As a general exploratory analysis of the distribution of QTL effects, we first performed separate multivariate ordinations of the **a** and **d** vectors by principal component analysis (PCA; *e.g.*, Jolliffe 2002). These PCAs were based on the covariance matrices of the **a** and **d** vectors, using the QTL as observations and the landmark coordinates as the variables, and therefore maintained the geometry and distances of shape tangent space (Rohlf 1999). Because the QTL effects are defined as vectors of genotypic differences, we used the uncentered **a** and **d** vectors to compute covariance matrices and principal component (PC) scores (the difference to the standard centered covariance matrices was small, because the means of **a** and **d** vectors were very close to zero). The resulting plots of PC scores are therefore simply a projection of the QTL effects on those axes that account for the maximal amount of variation among QTL and provide an optimal summary of the total variation in few dimensions. Because the PCs are directions in shape space, specific shape changes are associated with them, which can be displayed graphically and represent those features of shape that vary the most among the QTL.

The degree of clustering of QTL effects in shape tangent space was quantified by the *k*-means clustering method and tested statistically with a parametric bootstrap approach (Klingenberg *et al.* 2001). The *k*-means clustering algorithm searches for the partition of a sample of multivariate observations into a number of groups (g) that minimizes the total sum of squares within groups (or equivalently, the ratio of the total within-group sum of squares to the overall total sum of squares; *e.g.*, Krzanowski and Marriott 1995, p. 80). We ran *k*-means clustering analyses for $g = 2$ and $g = 3$, and we used the ratio of the within-cluster sum of squares to the overall total sum of squares as the measure for the degree of clustering (these sums of squares were the totals over all coordinates; *cf.* Klingenberg and McIntyre 1998). The results of these analyses were tested against the null hypothesis of a completely homogeneous distribution of the **a** or **d** vectors. The parametric bootstrap test (Efron and Tibshirani 1993) simulated this null hypothesis with a multivariate normal distribution with a covariance matrix that had the same eigenvalues as the covariance matrix for the respective QTL effects (Klingenberg *et al.* 2001). These simulated data were then entered into the *k*-means cluster analysis for $g = 2$ and $g = 3$, and the ratio of the within-cluster total sum of squares to the overall total sum of squares was compared to the original data for 1000 simulation rounds.

Covariation between parts of the mandible: A different way to address the question of modularity is the covariation between landmarks in different parts of the mandible. To the extent that modules are distinct from each other, there should be only relatively little covariation between them or, in the extreme, they would be completely independent of one another. In contrast, a morphological structure that consists of a single integrated module would show high covariation between all its parts (Klingenberg and Zaklan 2000).

To quantify the covariation between subsets of landmarks, we used the squared trace correlation, which is a measure of association between two sets of variables (Hooper 1959; Mardia *et al.* 1979, pp. 170–171). This statistic can take values between the extremes of zero for sets of variables that are completely independent and one for sets of variables that are totally redundant. The squared trace correlation can be viewed as a multivariate analog to the coefficient of determination familiar from univariate statistics, as it indicates the proportion of total variance in one set of variables for which the other set can account (Hooper 1959).

We assessed the statistical significance of covariation between modules with a randomization test (Good 1994; Edgington 1995), which simulated the null hypothesis of independence between modules by randomly exchanging the two subsets of landmarks among QTL for each of 10,000 permutation steps (Klingenberg and Zaklan 2000; Klingenberg *et al.* 2003). Because the Procrustes fit superimposes all the landmark configurations, localized variation can be spread to other parts of the configuration (*e.g.*, critiques of Walker 2000; Lele and Richtsmeier 2001) and potentially inflate the covariation between modules. These possible effects of the Procrustes superimposition were taken into account by including a new Procrustes fit in each permutation step (Klingenberg *et al.* 2003). For this purpose, the mean shape vector was added to the vectors of QTL effects before the permutation test, because the mean shape is important for the Procrustes fit, but does not affect the computation of the trace correlation. For each step, the two sets of landmarks were exchanged among QTL randomly, the resulting combined shapes were subjected to a Procrustes fit, and the squared trace correlation between modules was computed from the superimposed data and compared to the original value (Klingenberg *et al.* 2003). This analysis was carried out separately for the additive and dominance effects.

Comparisons of alternative partitions: A further approach to test modularity in the QTL effects and the hypothesized location of the boundary between modules was based on the relative strength of covariation of landmark positions between different subsets of landmarks (Klingenberg *et al.* 2003). Within each module, developmental interactions are expected to produce strong covariation among its component parts, whereas the relative independence of modules will result in weaker covariation between parts that belong to different modules (Cheverud 1996; Klingenberg 2004). Therefore, if a structure consists of two separate modules and the total set of landmarks is divided into subsets accordingly, covariation of landmark positions between these subsets should be relatively weak. In contrast, if the structure is partitioned in a manner that does not correspond to the boundary between its modules, the strong covariation within modules will contribute to the covariation between these subsets, which therefore will be greater than that for the partition that corresponds to the true subdivision into modules. Therefore, it is possible to test the hypothetical boundary between modules by a comparison of alternative partitions of a structure into subsets of landmarks (Klingenberg *et al.* 2003). Of all possible partitions, the division corresponding to the true boundary between modules should yield the minimum covariation between subsets.

We computed the trace correlation for all 6435 possible partitions of the mandible into two subsets of eight landmarks and computed the trace correlation between subsets for each of them. These partitions included many that divided the landmarks into subsets that were not spatially contiguous and therefore may not be a biologically realistic base of comparison for assessing modularity. Developmental modules have often been related to the concept of embryonic fields (*e.g.*, Davidson 1993; Gilbert *et al.* 1996; Wilkins 2002, pp. 255–258), which are spatially delimited units of patterning involving signaling interactions. Because modules in this sense need to be contiguous, we made separate comparisons exclusively for spa-

tially contiguous subsets of landmarks. Because all the landmarks used in this study are arranged around the outline of the mandible (Figure 1), we compared all partitions of the mandible in two subsets of eight landmarks each that were contiguous along the outline.

RESULTS

QTL for shape: The analyses located 33 QTL that affected mandible shape, most of which were statistically significant at the genome-wide level (Table 1). These were distributed over all the autosomes, except for chromosome 3.

The QTL effects displayed a variety of shape changes (Figure 2). Most of these shape changes consisted of a combination of relative shifts of neighboring landmarks relative to one another, often in opposite directions, and therefore tend to be combinations of shape changes at a small spatial scale, rather than global deformations of the whole mandible. Comparisons of the diagrams of QTL effects (Figure 2) suggest that most QTL appear to be distinct in terms of their effects on overall mandible shape, and there are no groups of QTL with similar effects on shape. Moreover, comparison of the additive and dominance effects of the QTL indicates that there is also no clear association between them; that is, the additive and dominance effects of a given QTL appear to be as different from each other as they are from the corresponding effects of different QTL.

Comparison of landmark shifts in different regions of the mandible indicated that QTL effects tended to be strongest for the landmarks of the ascending ramus and particularly for those in the condylar and coronoid processes (Figure 2). In the condyle, both the arrangement of the three landmarks in the condylar head and the overall length of the condyle varied. For the coronoid process, variation concerned both its length and arrangement in relation to neighboring parts of the mandible. There was also variation in the direction and robustness of the angular process, in the shape of the lower contour of the mandible, and in the arrangement of the incisor and molar alveoli.

For all but a few QTL, there were simultaneous changes in most parts of the mandible, and a clear division into anterior and posterior modules was not immediately apparent from the shape changes corresponding to these QTL effects (Figure 2). Artifacts from the Procrustes fit can be ruled out as a possible origin of these simultaneous effects, because the effects are mostly combinations of various small-scale shape changes and not shifts of single landmarks or small sets of landmarks against the rest of the configuration.

Ordinations and tests for clustering of QTL effects: The first two PCs accounted for 40.9 and 38.6% of the total variation in the analyses of the additive and dominance effects, respectively. They are therefore a fairly effective, although not complete, summary of the total 28-dimensional variation in just 2 dimensions. The shape features associated with the first two PCs concerned primarily the ascending ramus, with various changes in the relative sizes and arrangement of the mandibular processes, in particular the condyle and coronoid process (Figure 3, insets). Plots of PC scores showed a considerable amount of variation among QTL, but they provided no evidence for structured variation that would suggest distinct groups of QTL affecting different parts of the mandible (Figure 3).

The statistical tests of clustering into two or three groups did not provide evidence for structured variation among the **a** and **d** vectors of the QTL. For the additive effects, the ratios of within-groups sums of squares to the overall total sums of squares were 0.835 for $g = 2$ ($P = 0.95$) and 0.717 for $g = 3$ ($P = 0.92$). For the dominance effects, the ratios were 0.831 for $g = 2$ ($P = 0.88$) and 0.743 for $g = 3$ ($P = 0.97$). These results indicate that the largest portion of the total variation was within the groups of QTL and not among groups, and the parametric bootstrap tests consistently suggested that the tendency of QTL to fall into two or three groups was no stronger than would be expected for completely homogeneous data. Overall, therefore, there is no evidence for clustering among the QTL with respect to their effects on distinct parts of the mandible.

Covariation between modules: The covariation between the alveolar region and the ascending ramus was quantified by their squared trace correlation, which was 0.584 for the additive QTL effects and 0.571 for the dominance effects. The permutation test, which included the step of Procrustes refitting in the permutation routine, produced a nonsignificant result both for the additive QTL effects ($P = 0.29$) and for the dominance effects ($P = 0.52$).

The association between the alveolar region and ascending ramus for the QTL effects substantially exceeded that for phenotypic variation, which had a squared trace correlation of 0.294 ($P < 0.0001$ in the permutation test with Procrustes refitting). This weaker correlation indicates that the separation of modules is more marked at the phenotypic level and suggests that factors other than these QTL contribute to uncorrelated variation in the two parts of the mandible. Moreover, this phenotypic correlation can serve as an upper bound for the possible bias resulting from the Procrustes superimposition, because the trace correlations for the QTL effects and the phenotypic trace correlation were computed on the basis of the same Procrustes fit.

Comparison of alternative partitions of the mandible: To localize the boundary between modules in the mandible, we compared the covariation between the alveolar region and the ascending ramus to the covariation for other possible partitions of the mandible in two subsets of eight landmarks each. The expectation was that the covariation between the true modules should be lower than that between other partitions.

TABLE 1

QTL analysis for shape

QTL	LOD	Proximal marker	Marker distance	Marker C.I.	Centromere distance	Centromere C.I.	Additive magnitude $\|\|\mathbf{a}\|\|$	Dominance magnitude $\|\|\mathbf{d}\|\|$
QTL-SH1.1	21.19**	*D1Mit74*	12	*D1Mit74* + 8–*D1Mit7* + 6	53	49–61	0.00342**	0.00250
QTL-SH1.2		*D1Mit11*	16	*D1Mit11* + 12–*D1Mit11* + 22	83	79–89	0.00462**	0.00320
QTL-SH2.1	14.54**	*D2Mit1*	28	*D2Mit1* + 0^{end}–*D2Mit37* + 8	29	1–55	0.00380**	0.00388
QTL-SH2.2		*D2Mit38*	12	*D2Mit38* + 6–*D2Mit38* + 18	81	75–87	0.00502**	0.00400
QTL-SH4.1	10.15**	*D4Mit17*	6	*D4Mit163* + 10–*D4Mit17* + 12	45	33–51	0.00429**	0.00374
QTL-SH4.2		*D4Mit16*	4	*D4Mit45* + 6–*D4Mit13* + 0^{end}	79	59–97	0.00292**	0.00291
QTL-SH5.1	6.38**	*D5Mit61*	44	*D5Mit61* + 28–*D5Mit6* + 6	65	49–83	0.00318	0.00498**
QTL-SH5.2		*D5Mit26*	8	*D5Mit26* + 0–*D5Mit26* + 24	95	87–111	0.00348*	0.00532**
QTL-SH6.1	15.65**	*D6Mit1*	24	*D6Mit1* + 0^{end}–*D6Mit1* + 40	27	3–43	0.00516**	0.00424
QTL-SH6.2		*D6Mit58*	2	*D6Nds5* + 4–*D6Mit15* + 0^{end}	97	77–101	0.00443**	0.00192
QTL-SH7.1	10.72**	*D7Nds1*	4	*D7Mit26* + 6–*D7Nds1* + 8	49	39–53	0.00415**	0.00257
QTL-SH7.2		*D7Mit9*	4	*D7Mit17* + 12–*D7Mit71* + 2	85	71–85	0.00266**	0.00252
QTL-SH8.1	12.03**	*D8Mit293*	22	*D8Mit293* + 8–*D8Mit8* + 12	43	29–57	0.00258**	0.00196
QTL-SH8.2		*D8Mit89*	6	*D8Mit8* + 20–*D8Mit89* + 12	103	65–109	0.00266**	0.00252
QTL-SH9.1^{M}	10.07**	*D9Mit4*	8	*D9Mit8* + 4–*D9Mit8* + 28	47	41–65	0.00413**	0.00411*
QTL-SH9.1^{F}	2.47*	*D9Mit19*	0	*D9Mit8* + 18–*D9Mit19* + 0^{end}	89	65–89	0.00406*	0.00481*
QTL-SH10.1	18.46**	*D10Mit2*	18	*D10Mit2* + 10–*D10Mit2* + 26	34	26–44	0.00367**	0.00448
QTL-SH10.2		*D10Mit133*	4	*D10Mit10* + 2–*D10Mit14* + 0^{end}	96	86–104	0.00464**	0.00303
QTL-SH11.1	14.13**	*D11Mit64*	4	*D11Mit64* + 2–*D11Mit64* + 6	52	50–54	0.00482**	0.00283
QTL-SH11.2		*D11Mit333*	6	*D11Mit14* + 10–*D11Mit333* + 14	106	94–114	0.00333**	0.00385
QTL-SH12.1	15.95**	*D12Mit37*	6	*D12Mit37* + 0^{end}–*D12Mit37* + 10	7	1–11	0.00440**	0.00342
QTL-SH12.2		*D12Mit6*	6	*D12Mit2* + 0–*D12Mit2* + 14	59	53–67	0.00402**	0.00304
QTL-SH13.1	3.78**	*D13Mit1*	8	*D13Mit1* + 0^{end}–*D13Mit15* + 46	9	1–57	0.00268**	0.00248
QTL-SH13.2		*D13Mit9*	20	*D13Mit9* + 6–*D13Mit35* + 0^{end}	83	69–99	0.00426**	0.00285
QTL-SH14.1	7.66**	*D14Mit5*	0	*D14Nds1* + 26–*D14Mit5* + 8	46	28–54	0.00216	0.00281**
QTL-SH14.2		*D14Mit7*	16	*D14Mit7* + 10–*D14Mit266* + 0^{end}	82	76–90	0.00327**	0.00338**
QTL-SH15.1	9.93**	*D15Mit5*	2	*D15Mit13* + 6–*D15Mit5* + 16	33	13–47	0.00263**	0.00220
QTL-SH15.2		*D15Mit2*	10	*D15Mit2* + 2–*D15Mit2* + 18	67	59–75	0.00367**	0.00331
QTL-SH16.1	5.54**	*D16Mit2*	20	*D16Mit2* + 12–*D16Mit5* + 0^{end}	34	26–44	0.00288**	0.00359
QTL-SH17.1	6.20**	*D17Mit46*	8	*D17Mit46* + 4–*D17Mit16* + 0	20	16–22	0.00316**	0.00251
QTL-SH18.1	14.41**	*D18Mit17*	8	*D18Mit12* + 2–*D18Mit17* + 16	29	19–37	0.00283**	0.00321
QTL-SH18.2		*D18Mit79*	0	*D18Mit51* + 8–*D18Mit79* + 0^{end}	63	51–63	0.00249**	0.00247
QTL-SH19.1	2.31*	*D19Mit2*	6	*D19Mit14* + 6–*D19Mit137* + 0^{end}	75	37–81	0.00225**	0.00182

Values are the locations, confidence intervals (C.I.), and the magnitudes of the additive ($\|\|\mathbf{a}\|\|$) and dominance effects ($\|\|\mathbf{d}\|\|$) of all QTL affecting shape. Each QTL is designated as "QTL-SH" followed by its chromosome number and an extension of 1 or 2 to indicate whether it was the first or second QTL on that chromosome and by the superscript "M" or "F" if it specifically affected either males or females. Locations and confidence intervals are given as map distances from the nearest proximal marker and from the centromere, with the superscript "end" denoting a confidence interval truncated at the position of an extreme marker. All LOD scores are significant at the 5% (*) or 1% (**) chromosome-wide level, and those underlined are significant at the 5% genome-wide level.

Of all 6435 possible partitions of the mandible into two groups of eight landmarks, the trace correlation was equal to or less than the observed value 167 times for the additive effects (2.60%) and 7 times for the dominance effects (0.11%). For the phenotypic shape variation, which results from the aggregate effects of all QTL and of environmental variation, the division into the alveolar region and the ascending ramus yielded a lower squared trace correlation than did any of the other partitions. These results clearly indicate that the observed trait correlations are in the lower tail of the distribution of this statistic for all possible partitions and therefore provide support for the hypothesized location of the boundary between modules. It should be noted, however, that the percentages indicated above should not be interpreted formally as *P* values for a statistical test, because the many partitions in which the landmarks are broken up into subsets that are not spatially contiguous may not represent a null hypothesis that is biologically realistic (*e.g.*, if modules are associated with embryonic fields).

We separately compared the squared trace correlations among just those alternative partitions that divided the mandible into two subsets that were contiguous along the outline of the mandible (Figure 4). For the additive QTL effects, there was one partition with a squared trace correlation of 0.583 that was minimally lower than the value of 0.584 for the partition into alveolar region and ascending ramus. For the dominance effect, the *a priori* partition into alveolar region and ascending ramus yielded the weakest covariation. For both the additive and dominance QTL effects, the range of values of the squared trace correlation was fairly small, indicating that modularity of QTL effects is a matter of degrees, rather than a contrast of complete integration within modules and independence between them.

DISCUSSION

The results of our analyses confirm and refine the findings of previous studies that have reported a modular structure of pleiotropic QTL effects on the morphology of the mouse mandible. Most previous studies on this subject have investigated the spatial distribution of statistically significant QTL effects on distance measurements in the mandible (Bailey 1985, 1986; Cheverud *et al.* 1997; Mezey *et al.* 2000; Ehrich *et al.* 2003). This study uses a complementary approach, employing geometric morphometrics to quantify QTL effects on the shape of the mandible in direct relation to its anatomical structure (Klingenberg *et al.* 2001). Here we have extended this methodology to investigate modularity and integration through multivariate analyses of QTL effects and their joint variation within and between the modules of the mandible.

Spatial patterns of QTL effects: The geometric methods used in this study are particularly suited to visualize the QTL effects directly by graphical displays of the corresponding shape changes (Figure 2; see also Klingenberg *et al.* 2001; Workman *et al.* 2002). These diagrams show a diversity of patterns of landmark shifts, which vary in the degree to which they are localized to specific parts or spread over the entire mandible, in the directions of landmark changes, and in the combinations of the changes in different parts of the mandible.

In comparison to our previous analysis (Klingenberg *et al.* 2001), this greater diversity appears to be the result of the greatly improved spatial coverage of landmarks (16 landmarks instead of 5). The recurrent patterns observed for many of the QTL in the earlier study, an opposite relative shift of the coronoid and angular processes in the anterior-posterior direction and a dorsoventral compression or extension of the same two processes, can still be seen as part of many QTL effects and in the shape changes associated with the principal components of QTL effects (Figure 3), but they occur in combination with other changes that often are considerably stronger (*e.g.*, variation in the condylar process). Moreover, these large-scale deformations of the whole mandible are overlaid with localized movements of neighboring landmarks against each other, which correspond to anatomically localized expansions or contractions of mandibular parts. These combinations of effects appear to give each QTL a fairly distinctive pattern.

There may be a different set of recurrent patterns in the QTL effects, but these seem to concern smaller units of the mandible, such as the three processes of the ascending ramus or portions of the alveolar region each on its own, rather than the mandible as a whole. This level of the organization of the mandible, corresponding to distinct embryological origins and with different schedules of differentiation, has been emphasized in earlier studies of morphological variation in the mandible (Atchley and Hall 1991; Köntges and Lumsden 1996; Miyake *et al.* 1997; Tomo *et al.* 1997; Ramaesh and Bard 2003). Because our data set contains only two or three landmarks for each of these units, however, the spatial resolution is again a factor limiting our ability to distinguish whether these are indeed recurring elements of shape change in the mandible or whether each individual QTL produces characteristic effects in all these units. The answer to this question is of interest because it would indicate whether these morphological units behave as autonomous and coherent modules in terms of their contributions to the overall QTL effects.

The possibility exists that some of the QTL effects found in this analysis are not the effects of a single locus, but the aggregate effect of two or more QTL in close linkage. This problem is not unique to multivariate QTL studies, as it has been known from univariate studies (*e.g.*, Flint and Mott 2001; Mackay 2001), but it is of particular concern for studies of integration because it

brings with it the potential to confound the analysis of the patterns of QTL effects. In particular, the apparent individuality of QTL effects might in part be due to various combinations of simpler QTL effects, and genetic linkage between loci with effects on different modules might lead to a systematic underestimate of the separation of the modules. A possibility to address this problem in future studies is to use experimental designs that have greater genetic resolution, such as advanced intercross lines (Darvasi and Soller 1995) or heterogeneous stocks (Talbot *et al.* 1999; Mott *et al.* 2000). Application of these more powerful methods will also increase the number of QTL detected and thereby improve the power of statistical tests. We are optimistic that these new approaches will overcome current methodological problems and will allow sensitive tests of the question of whether there is individuality of QTL effects or whether there are classes of QTL, perhaps corresponding to sets of genes with related function in mandible development (*e.g.*, Depew *et al.* 2002a; Cobourne and Sharpe 2003).

Modularity of pleiotropic QTL effects: We used multivariate methods to test the hypothesis that QTL effects on shape reflect the modular structure of the mandible. First, we examined whether distinct sets of QTL affecting the traits in the alveolar region and ascending ramus are recognizable as distinct clusters according to their effects on shape. Second, we quantified covariation among landmark positions between the hypothesized modules, because true modules should correspond to a partition of the mandible into subsets that have minimal covariation between each other. These are two distinct but complementary aspects of modularity in QTL effects, the first one focusing on the arrangement of QTL in the multidimensional shape space and the second one emphasizing the expectation of relative independence between modules.

No evidence for clustering of the QTL effects was found in the multivariate ordination by principal component analysis (Figure 3). Because it was not entirely clear from previous studies whether the hypothesis of modularity predicts two clusters of QTL affecting the two modules separately or whether there may be an additional third cluster of QTL with effects on both modules simultaneously, we included both these possibilities in the formal test for clustering. However, the parametric bootstrap tests did not provide any support for either version of this hypothesis, as the degree of clustering was just as strong in purely homogeneous random data as among the QTL effects. This result matches that of our earlier study with fewer landmarks (Klingenberg *et al.* 2001), suggesting that the failure of that analysis to find distinct groups of QTL with different effects on mandible shape was not merely a consequence of insufficient spatial resolution. Likewise, analyses of the localization and strength of QTL effects on distances between landmarks in the mandible indicate a multitude of different patterns (Bailey 1985, 1986; Cheverud *et al.* 1997; Ehrich *et al.* 2003). These results underscore that the QTL affecting shape variation in the alveolar region and the ascending ramus of the mandible are not homogeneous in their effects, but they are assemblages of loci whose effects are individually distinct but more or less concentrated in different regions of the mandible.

Covariation between the two modules of the mandible, as measured by the squared trace correlation among the positions of landmarks in the two sets, was difficult to assess. The values of 0.584 and 0.571 computed for the additive and dominance effects of the QTL were fairly high, indicating that more than half of the total variance was shared between modules. These correlations were not statistically significant in the permutation test that included an adjustment for the effects of the Procrustes fit. It is likely, however, that this is a consequence of the low statistical power of this test with the relatively small sample size of 33 QTL, which only slightly exceeds the 28 dimensions of the shape tangent space. In contrast, the phenotypic covariation between modules, computed over the 954 mice included in the study, was highly significant in the same statistical test, even though the value of the squared trace correlation was only 0.294. Altogether, these results point toward a moderate degree of covariation of QTL effects between the two modules. It follows that the QTL are not divided neatly into groups of loci whose effects are limited to either the alveolar region or the ascending ramus, but there is a tendency for the effects of QTL to be stronger in one or the other of the two modules.

As a test of the hypothesized location of the modular boundary between the alveolar region and the ascending ramus, we compared the covariation among alternative partitions of the mandible. This test provided evidence in favor of the hypothesis. The trace correlations computed for QTL effects were clearly in the left tail of the distribution of the same statistic for all possible partitions of the mandible. The comparisons that included only the partitions of the mandible into contiguous subsets gave a somewhat ambiguous result for the additive effects because two different partitions yielded

Figure 2.—QTL effects on shape. For each QTL, the additive effect (top) and dominance effect (bottom) are indicated as shape transformations from the overall average shape (open circles and gray outline) to the shape with the respective effect added (solid circles and black outline). Because the QTL effects are subtle, all effects have been amplified 25-fold for better visibility. The changes of outlines are interpolated from the information on the landmark shifts with the thin-plate spline method (Bookstein 1989).

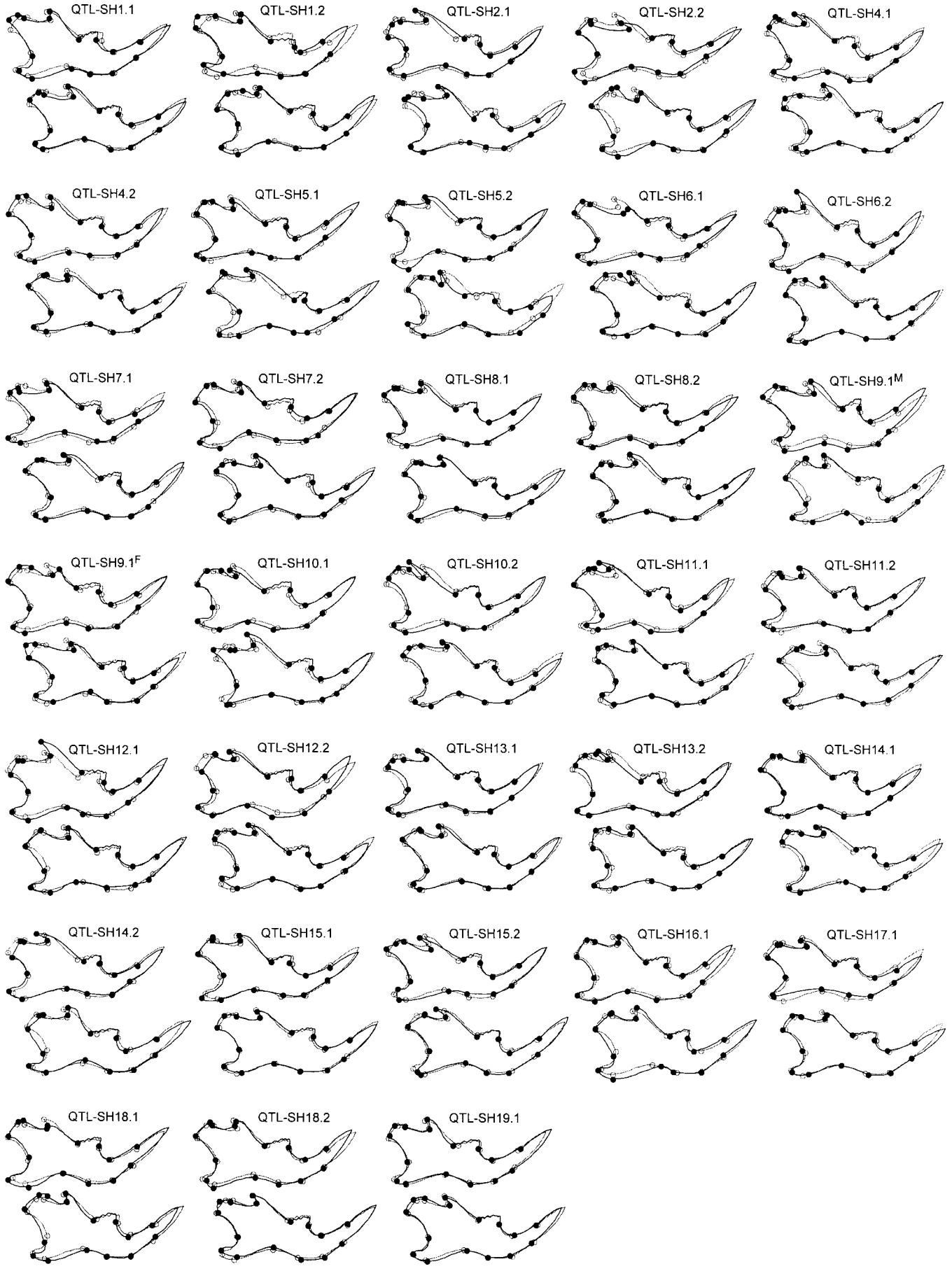
QTL-SH1.1
QTL-SH1.2
QTL-SH2.1
QTL-SH2.2
QTL-SH4.1
QTL-SH4.2
QTL-SH5.1
QTL-SH5.2
QTL-SH6.1
QTL-SH6.2
QTL-SH7.1
QTL-SH7.2
QTL-SH8.1
QTL-SH8.2
QTL-SH9.1M
QTL-SH9.1F
QTL-SH10.1
QTL-SH10.2
QTL-SH11.1
QTL-SH11.2
QTL-SH12.1
QTL-SH12.2
QTL-SH13.1
QTL-SH13.2
QTL-SH14.1
QTL-SH14.2
QTL-SH15.1
QTL-SH15.2
QTL-SH16.1
QTL-SH17.1
QTL-SH18.1
QTL-SH18.2
QTL-SH19.1

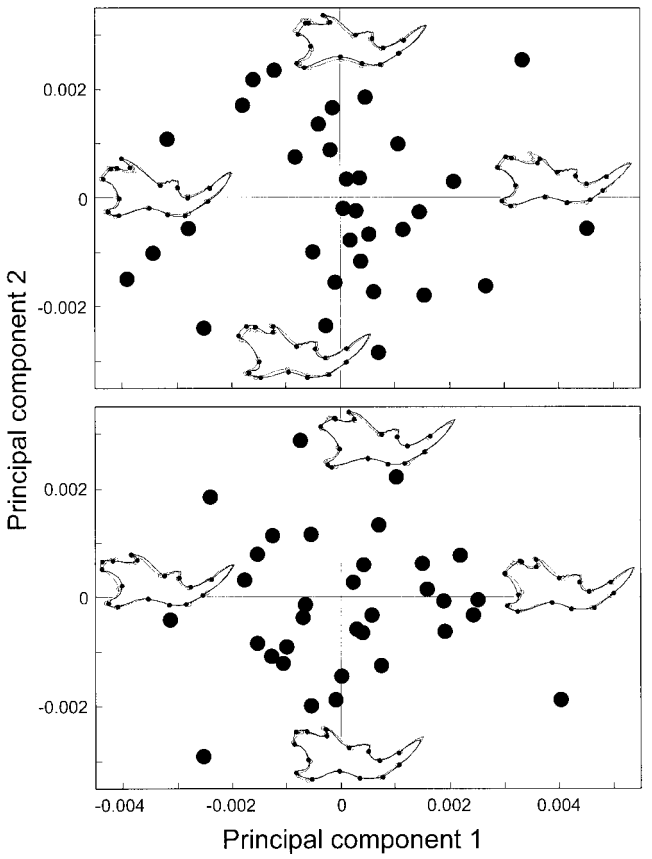

FIGURE 3.—Multivariate ordination of QTL effects by PC analysis. The first two PCs for the additive (top) and dominance effects (bottom) are shown, and the insets illustrate the shape changes associated with the PCs along each one of the axes in positive and negative directions.

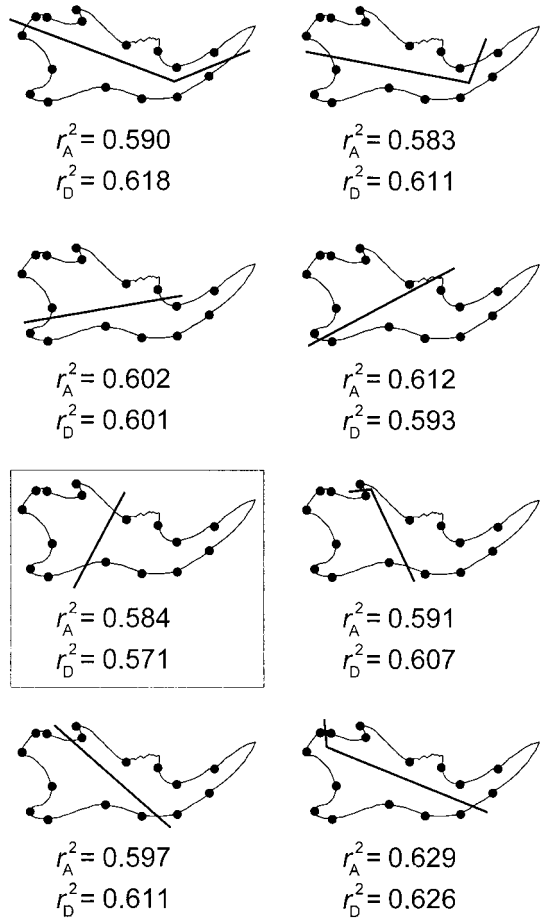

FIGURE 4.—Comparison of covariation among alternative partitions of the mandible into two subsets of eight landmarks each. The diagrams show all such partitions that divide the landmarks into subsets that are contiguous along the outline of the mandible. The values are the squared trace correlations between subsets of landmarks for the additive (r_A^2) and dominance (r_D^2) effects of the QTL. The boxed diagram indicates the *a priori* partition of the mandible into alveolar region and ascending ramus (*cf.* Figure 1).

nearly the same low trace correlation (Figure 4), but for the dominance effects the hypothesized division yielded the lowest amount of covariation. Some of the uncertainty in these analyses of covariance patterns may be due to the small sample size and high-dimensional variation (33 QTL for a 28-dimensional shape tangent space) as well as sampling error in the estimates of QTL effects. It may therefore be no accident that the result for the phenotypic level of variation was much more clear-cut in this data set (sample size 954) and in a similar study of phenotypic variation (sample size 90; KLINGENBERG *et al.* 2003). Overall, these results confirm the hypothesis that the covariation of QTL effects between the alveolar region and the ascending ramus is weaker than the covariation between arbitrary subsets of landmarks.

In all these comparisons, the range of values for the squared trace correlation was fairly narrow, suggesting that alternative partitions of the mandible differ in the amount of covariation between subsets, but not just in the presence or absence of such covariation. The alveolar region and ascending ramus are fairly coherent internally and relatively autonomous from each other, but that does not mean that each module would be completely homogeneous and independent of the other one. QTL have manifold localized effects on smaller units within the two main modules, because positions of neighboring landmarks shift relative to each other, and most QTL show a certain degree of overall integration in that they affect most parts of the mandible at least to some degree (Figure 2). In other words, for geometric shape in the mouse mandible, our results show that modularity is not complete, either in terms of integration within modules or in terms of parcellation between modules (WAGNER 1996; WAGNER and ALTENBERG 1996; MEZEY *et al.* 2000).

Overall, these results indicate that modularity of QTL effects is a question of degrees rather than a black-or-white issue. These findings suggest a shift of perspective from the dichotomy of QTL "with effects" or "without effects" on sets of traits to an approach in which the effects of all QTL on the complete set of traits are quantified. Whereas simplified binary representations

clearly have great advantages as heuristic models (*e.g.*, Gromko 1995), they are unlikely to yield adequate characterizations of real biological systems. Considering QTL effects in a quantitative manner is an inherently more complex task, but in return such an approach will provide a richer and more subtle picture of the genetic systems controlling morphological variation in real organisms.

Developmental origin of pleiotropic effects: These results concerning the modularity of QTL effects are comparable to those obtained in a study that used analysis of correlated asymmetry to infer the developmental origin of covariation among landmarks in the mouse mandible (Klingenberg *et al.* 2003). Although this inference is based explicitly on variation from a nongenetic source, the resulting information on the developmental basis of this variation can also be used to understand the origin of pleiotropic effects of genes involved in the system.

Two broad classes of mechanisms that give rise to covariation of morphological traits can be distinguished (Klingenberg 2003, 2004). On the one hand, covariation can originate from direct interactions between the developmental pathways that produce the traits of interest. Examples of this class include the partitioning of a precursor tissue into two or more structures or inductive signaling from one tissue to another (*e.g.*, Riska 1986; Wilkins 2002). These interactions are often spatially localized in morphogenetic fields (Davidson 1993, 2001; Carroll *et al.* 2001), which can be interpreted as the embryonic precursors of morphological modules. An important characteristic of covariation from direct developmental interaction is that variation is directly transmitted from one pathway to another, and the effects of perturbations from within the pathway can be passed along to be expressed in multiple "downstream" traits simultaneously. A fundamentally different origin of morphological covariation is the parallel variation of separate pathways in response to variation in environmental conditions or to allelic variation in a gene involved in multiple pathways (Klingenberg 2003, 2004). For instance, many genes play critical roles in multiple developmental processes (Davidson 2001; Wilkins 2002) and therefore have the potential to cause simultaneous effects on these pathways that produce parallel variation in them. It is important to note that the mechanism of parallel variation cannot transmit variation from within one of the pathways to the other (Klingenberg 2003, 2004).

To distinguish these two origins of covariation, external sources of variation should be eliminated by controlling rigorously against environmental and genetic variation, which eliminates parallel variation of separate pathways and leaves only covariation resulting from direct interaction (Klingenberg 2003). Perhaps the easiest way to achieve this is to focus on fluctuating asymmetry, small random differences between the left and right sides of animals that share the same genome and usually experience very similar environmental conditions. Because these asymmetries originate from random perturbations arising within the developmental system, correlations of asymmetries must be based exclusively on direct interactions between developmental pathways and not on parallel variation (Klingenberg 2003).

A study of correlations in the asymmetries of distance measurements in the mouse mandible found that asymmetries were more strongly correlated within the alveolar region and the ascending ramus than between them (Leamy 1993), indicating that direct developmental interactions take place primarily within the two modules. An analysis of shape asymmetry that used the same methods and a similar set of landmarks as in the present study obtained results that are directly comparable to those of this analysis of QTL effects (Klingenberg *et al.* 2003). Covariation between the alveolar region and ascending ramus was moderate for both asymmetry and variation among individuals (squared trace correlations near 0.4). The comparison of alternative partitions yielded the lowest squared trace correlations for the hypothesized modular boundary and showed that the values of the squared trace correlation between subsets varied over a limited range for the alternative partitions. Overall, the patterns of covariation for asymmetry broadly agree with those found in the present analysis for QTL effects in that they show an intermediate degree of modularity and indicate the same location of the boundary between modules. This correspondence of patterns raises the possibility that the interactions among developmental pathways, which produce the covariation of asymmetry, also may be the mechanisms that shape the modular patterns of QTL effects.

Determining the precise mechanisms that generate pleiotropic effects of individual QTL will require the identification of the genes responsible (Flint and Mott 2001; Mackay 2001) as well as an understanding of the epigenetic processes that translate allelic variation of those genes into the observed phenotypic effects (Atchley and Hall 1991; Hall 1999; Depew *et al.* 2002b; Cobourne and Sharpe 2003; Ramaesh and Bard 2003). While it is not possible to make inferences on the mechanism involved in the case of any single QTL without such detailed information, the similarity of the patterns of QTL variation found in this study to those for covariation of asymmetry (Klingenberg *et al.* 2003) suggests that, in the aggregate, direct developmental interactions are responsible for a considerable proportion of the patterns of genic variation. Information on those developmental interactions will therefore be of crucial importance for understanding QTL effects and the evolution of genetic architecture.

LITERATURE CITED

Atchley, W. R., and B. K. Hall, 1991 A model for development and evolution of complex morphological structures. Biol. Rev. **66:** 101–157.

Bailey, D. W., 1985 Genes that affect the shape of the murine mandible: congenic strain analysis. J. Hered. **76:** 107–114.

Bailey, D. W., 1986 Genes that affect morphogenesis of the murine mandible: recombinant-inbred strain analysis. J. Hered. **77:** 17–25.

Bookstein, F. L., 1989 Principal warps: thin-plate splines and the decomposition of deformations. IEEE Trans. Patt. Anal. Mach. Intell. **11:** 567–585.

Bookstein, F. L., 1991 *Morphometric Tools for Landmark Data: Geometry and Biology*. Cambridge University Press, Cambridge, UK.

Bookstein, F. L., 1996 Combining the tools of geometric morphometrics, pp. 131–151 in *Advances in Morphometrics*, edited by L. F. Marcus, M. Corti, A. Loy, G. J. P. Naylor and D. E. Slice. Plenum Press, New York.

Carroll, S. B., J. K. Grenier and S. D. Weatherbee, 2001 *From DNA to Diversity: Molecular Genetics and the Evolution of Animal Design*. Blackwell Science, Malden, MA.

Chai, Y., X. Jiang, Y. Ito, P. Bringas, Jr., J. Han *et al.*, 2000 Fate of the mammalian cranial neural crest during tooth and mandibular morphogenesis. Development **127:** 1671–1679.

Cheverud, J. M., 1982 Phenotypic, genetic, and environmental morphological integration in the cranium. Evolution **36:** 499–516.

Cheverud, J. M., 1995 Morphological integration in the saddle-back tamarin (*Saguinus fuscicollis*) cranium. Am. Nat. **145:** 63–89.

Cheverud, J. M., 1996 Developmental integration and the evolution of pleiotropy. Am. Zool. **36:** 44–50.

Cheverud, J. M., S. E. Hartman, J. T. Richtsmeier and W. R. Atchley, 1991 A quantitative genetic analysis of localized morphology in mandibles of inbred mice using finite element scaling. J. Craniofac. Genet. Dev. Biol. **11:** 122–137.

Cheverud, J. M., E. J. Routman, F. A. M. Duarte, B. van Swinderen, K. Cothran *et al.*, 1996 Quantitative trait loci for murine growth. Genetics **142:** 1305–1319.

Cheverud, J. M., E. J. Routman and D. J. Irschick, 1997 Pleiotropic effects of individual gene loci on mandibular morphology. Evolution **51:** 2006–2016.

Churchill, G. A., and R. W. Doerge, 1994 Empirical threshold values for quantitative trait mapping. Genetics **138:** 963–971.

Cobourne, M. T., and P. T. Sharpe, 2003 Tooth and jaw: molecular mechanisms of patterning in the first branchial arch. Arch. Oral Biol. **48:** 1–14.

Darvasi, A., and M. Soller, 1995 Advanced intercross lines, an experimental population for fine genetic mapping. Genetics **141:** 1199–1207.

Davidson, E. H., 1993 Later embryogenesis: regulatory circuitry in morphogenetic fields. Development **118:** 665–690.

Davidson, E. H., 2001 *Genomic Regulatory Systems: Development and Evolution*. Academic Press, San Diego.

Depew, M. J., T. Lufkin and J. L. R. Rubenstein, 2002a Specification of jaw subdivisions by *Dlx* genes. Science **298:** 381–385.

Depew, M. J., A. S. Tucker and P. T. Sharpe, 2002b Craniofacial development, pp. 421–498 in *Mouse Development: Patterning, Morphogenesis, and Organogenesis*, edited by J. Rossant and P. P. L. Tam. Academic Press, San Diego.

Dryden, I. L., and K. V. Mardia, 1998 *Statistical Analysis of Shape*. Wiley, Chichester, UK.

Edgington, E. S., 1995 *Randomization Tests*. Marcel Dekker, New York.

Efron, B., and R. J. Tibshirani, 1993 *An Introduction to the Bootstrap*. Chapman & Hall, New York.

Ehrich, T. H., T. T. Vaughn, S. F. Koreishi, R. B. Linsey, L. S. Pletscher *et al.*, 2003 Pleiotropic effects on mandibular morphology I. Developmental morphological integration and differential dominance. J. Exp. Zool. Mol. Dev. Evol. **296B:** 58–79.

Falconer, D. S., and T. F. C. Mackay, 1996 *Introduction to Quantitative Genetics*. Longman, Essex, UK.

Ferguson, C. A., A. S. Tucker and P. T. Sharpe, 2000 Temporospatial cell interactions regulating mandibular and maxillary arch patterning. Development **127:** 403–412.

Flint, J., and R. Mott, 2001 Finding the molecular basis of quantitative traits: successes and pitfalls. Nat. Rev. Genet. **2:** 437–445.

Francis-West, P., R. Ladher, A. Barlow and A. Graveson, 1998 Signalling interactions during facial development. Mech. Dev. **75:** 3–28.

Gilbert, S. F., J. M. Opitz and R. A. Raff, 1996 Resynthesizing evolutionary and developmental biology. Dev. Biol. **173:** 357–372.

Good, P., 1994 *Permutation Tests: A Practical Guide to Resampling Methods for Testing Hypotheses*. Springer-Verlag, New York.

Gromko, M. H., 1995 Unpredictability of correlated response to selection: pleiotropy and sampling interact. Evolution **49:** 685–693.

Haley, C. S., and S. A. Knott, 1992 A simple regression method for mapping quantitative trait loci in line crosses using flanking markers. Heredity **69:** 315–324.

Hall, B. K., 1999 *Evolutionary Developmental Biology*. Kluwer, Dordrecht, The Netherlands.

Hooper, J. W., 1959 Simultaneous equations and canonical correlation theory. Econometrica **27:** 245–256.

Jansen, R. C., 1993 Interval mapping of multiple quantitative trait loci. Genetics **135:** 205–211.

Jolliffe, I. T., 2002 *Principal Component Analysis*. Springer-Verlag, New York.

Klingenberg, C. P., 2003 Developmental instability as a research tool: using patterns of fluctuating asymmetry to infer the developmental origins of morphological integration, pp. 427–442 in *Developmental Instability: Causes and Consequences*, edited by M. Polak. Oxford University Press, New York.

Klingenberg, C. P., 2004 Integration, modules and development: molecules to morphology to evolution, pp. 213–230 in *Phenotypic Integration: Studying the Ecology and Evolution of Complex Phenotypes*, edited by M. Pigliucci and K. Preston. Oxford University Press, New York.

Klingenberg, C. P., and L. J. Leamy, 2001 Quantitative genetics of geometric shape in the mouse mandible. Evolution **55:** 2342–2352.

Klingenberg, C. P., and G. S. McIntyre, 1998 Geometric morphometrics of developmental instability: analyzing patterns of fluctuating asymmetry with Procrustes methods. Evolution **52:** 1363–1375.

Klingenberg, C. P., and S. D. Zaklan, 2000 Morphological integration between developmental compartments in the *Drosophila* wing. Evolution **54:** 1273–1285.

Klingenberg, C. P., L. J. Leamy, E. J. Routman and J. M. Cheverud, 2001 Genetic architecture of mandible shape in mice: effects of quantitative trait loci analyzed by geometric morphometrics. Genetics **157:** 785–802.

Klingenberg, C. P., K. Mebus and J.-C. Auffray, 2003 Developmental integration in a complex morphological structure: How distinct are the modules in the mouse mandible? Evol. Dev. **5:** 522–531.

Knott, S. A., and C. S. Haley, 2000 Multitrait least squares for quantitative trait loci detection. Genetics **156:** 899–911.

Köntges, G., and A. Lumsden, 1996 Rhombencephalic neural crest segmentation is preserved throughout craniofacial ontogeny. Development **122:** 3229–3242.

Krzanowski, W. J., and F. H. C. Marriott, 1995 *Multivariate Analysis. Part 2. Classification, Covariance Structures and Repeated Measurements*. Arnold, London.

Lander, E. S., P. Green, J. Abrahamson, A. Barlow, M. Daley *et al.*, 1987 MAPMAKER: an interactive computer package for constructing primary genetic linkage maps of experimental and natural populations. Genomics **1:** 174–181.

Leamy, L., 1993 Morphological integration of fluctuating asymmetry in the mouse mandible. Genetica **89:** 139–153.

Leamy, L., and W. R. Atchley, 1984 Morphometric integration in the rat (*Rattus* sp.) scapula. J. Zool. **202:** 43–56.

Leamy, L. J., E. J. Routman and J. M. Cheverud, 1999 Quantitative trait loci for early- and late-developing skull characters in mice: a test of the genetic independence model of morphological integration. Am. Nat. **153:** 201–214.

Leamy, L. J., D. Pomp, E. J. Eisen and J. M. Cheverud, 2000 Quantitative trait loci for directional but not fluctuating asymmetry of mandible characters in mice. Genet. Res. **76:** 27–40.

Lele, S. R., and J. T. Richtsmeier, 2001 *An Invariant Approach to Statistical Analysis of Shapes*. Chapman & Hall/CRC, New York/Boca Raton, FL.

Lincoln, S., M. Daly and E. Lander, 1992 *Constructing Genetic Maps With MAPMAKER/EXP 3.0*. Whitehead Institute Technical Report, Whitehead Institute, Cambridge, MA.

Lynch, M., and B. Walsh, 1998 *Genetics and Analysis of Quantitative Traits*. Sinauer, Sunderland, MA.

Mackay, T. F. C., 2001 The genetic architecture of quantitative traits. Annu. Rev. Genet. **35:** 303–339.

Mardia, K. V., J. T. Kent and J. M. Bibby, 1979 *Multivariate Analysis.* Academic Press, London.

Mezey, J. G., J. M. Cheverud and G. P. Wagner, 2000 Is the genotype-phenotype map modular?: A statistical approach using mouse quantitative trait loci data. Genetics **156:** 305–311.

Miyake, T., A. M. Cameron and B. K. Hall, 1997 Stage-specific expression patterns of alkaline phosphatase during development of the first arch skeleton in inbred C57BL/6 mouse embryos. J. Anat. **190:** 239–260.

Mott, R., C. J. Talbot, M. G. Turri, A. C. Collins and J. Flint, 2000 A method for fine mapping quantitative trait loci in outbred animal stocks. Proc. Natl. Acad. Sci. USA **97:** 12649–12654.

Ramaesh, T., and J. B. L. Bard, 2003 The growth and morphogenesis of the early mouse mandible: a quantitative analysis. J. Anat. **203:** 213–222.

Riska, B., 1986 Some models for development, growth, and morphometric correlation. Evolution **40:** 1303–1311.

Rohlf, F. J., 1999 Shape statistics: Procrustes superimpositions and tangent spaces. J. Classif. **16:** 197–223.

Talbot, C. J., A. Nicod, S. S. Cherny, D. W. Fulker, A. C. Collins *et al.*, 1999 High-resolution mapping of quantitative trait loci in outbred mice. Nat. Genet. **21:** 305–308.

Tomo, S., M. Ogita and I. Tomo, 1997 Development of mandibular cartilages in the rat. Anat. Rec. **249:** 233–239.

Trainor, P. A., and P. P. L. Tam, 1995 Cranial paraxial mesoderm and neural crest cells of the mouse embryo: co-distribution in the craniofacial mesenchyme but distinct segregation in the branchial arches. Development **121:** 2569–2582.

Vaughn, T. T., L. S. Pletscher, A. Peripato, K. King-Ellison, E. Adams *et al.*, 1999 Mapping quantitative trait loci for murine growth: a closer look at genetic architecture. Genet. Res. **74:** 313–322.

Von Dassow, G., and E. Munro, 1999 Modularity in animal development and evolution: elements of a conceptual framework for EvoDevo. J. Exp. Zool. Mol. Dev. Evol. **285:** 307–325.

Wagner, G. P., 1996 Homologues, natural kinds and the evolution of modularity. Am. Zool. **36:** 36–43.

Wagner, G. P., and L. Altenberg, 1996 Complex adaptations and the evolution of evolvability. Evolution **50:** 967–976.

Walker, J. A., 2000 Ability of geometric morphometric methods to estimate a known covariance matrix. Syst. Biol. **49:** 686–696.

Weller, J. I., 2001 *Quantitative Trait Loci Analysis in Animals.* CABI Publishing, Wallingford, UK.

Wilkins, A. S., 2002 *The Evolution of Developmental Pathways.* Sinauer Associates, Sunderland, MA.

Workman, M. S., L. J. Leamy, E. J. Routman and J. M. Cheverud, 2002 Analysis of quantitative trait locus effects on the size and shape of mandibular molars in mice. Genetics **160:** 1573–1586.

Zeng, Z-B., 1994 Precision mapping of quantitative trait loci. Genetics **136:** 1457–1465.

Communicating editor: G. A. Churchill